CDC ROADM Design Tradeoffs due to Physical Layer Impairments in Optical Networks

Diogo Sequeira [a], Luís Cancela [a,b], João Rebola [a,b]

[a]*Instituto de Telecomunicações (IT), Lisbon, Portugal*
[b]*Dep. Information Science and Technology, Iscte - Instituto Universitário de Lisboa, Lisbon, Portugal*

Highlights

- The impact of physical layer impairments on CDC ROADM-based networks is assessed
- Multicast switches and WSSs are considered for the ROADM add/drop structures
- For 16QAM signals B&S ROADMs with WSSs-based add/drop structures is the best choice

---

Abstract

In this work, we assess the impact of several physical layer impairments (PLIs) on the performance of optical networks based on colorless, directionless and contentionless reconfigurable optical add/drop multiplexers (ROADMs), through Monte-Carlo simulation, and considering polarization division multiplexing 4 and 16 quadrature amplitude modulation (QAM) signals, at 28 GBaud, for 37.5 GHz optical channels. The PLIs taken into account are the amplified spontaneous emission noise, optical filtering, in-band crosstalk and nonlinear interference noise caused by Kerr effect. A detailed model of the ROADM node is built considering two typical ROADM architectures, broadcast and select (B&S) and route and select (R&S), and two different add/drop structures, multicast switches (MCSs) and wavelength selective switches (WSSs), resulting in four different ROADM node scenarios. Our results have shown that for 16QAM signals, the B&S ROADMs with WSSs-based add/drop structures is the scenario that has the best relation cost/performance, foreseeing its use in metro networks, while for 4-QAM signals, the R&S ROADM with WSSs-based add/drop structure scenario allows a larger ROADM cascade at an expectable lower cost anticipating its implementation in long-haul networks.

Keywords

coherent detection; CDC ROADMs; physical layer impairments; quadrature amplitude modulation; transparent optical networks.

Email addresses: dgsao@iscte-iul.pt (Diogo Sequeira), luis.cancela@iscte-iul.pt (Luís Cancela), joao.rebola@iscte-iul.pt (João Rebola)

December 5, 2020

1. Introduction

As the need for more capacity in optical transport networks has no signs of slowing down, as demanded by the emergent cloud and 5G services, different technological solutions aiming at increasing transport capacity have been being proposed in the recent years. Spatial division multiplexing (SDM) is seen as a promising solution to solve this capacity crunch, however, several SDM technology issues are still to be solved and so, SDM massive implementation is only foreseen as a future long-term solution [1].

The efficient usage of network resources, both transmission and switching resources, is a more auspicious solution to surpass this capacity crunch in the next coming years, especially from the operators' point of view due to cost constraints [1]. We have already witnessed enhanced spectrum efficiency in using a flexible grid, where, for example, Nyquist super channels or, more recently, elastic transponders capable of using a large set of modulation formats and baud rates can take full advantage of the available spectrum. Efficiency, in terms of dynamism and flexibility, is also very important to achieve in nowadays networks nodes. These nodes, known as reconfigurable optical add/drop multiplexers (ROADMs), have brought dynamism into the optical network level, since light-paths can now be configured very quickly by software, which is crucial for currently connection durations [2,3]. Route and select (R&S) and broadcast and select (B&S) ROADM architectures based on liquid crystal on silicon (LCoS) wavelength selective switches (WSS) are now two of the most commonly deployed ROADM architectures [4]. ROADM nodes have also brought flexibility to the network level since their add/drop (A/D) structures are now colorless, directionless and contentionless (CDC) [2,3,5]. This last feature means that the same wavelength can be used for different A/D operations in the same A/D structure, and together with the colorless and directionless features greatly contributes to simplify network planning and management. Typically, these A/D structures are implemented with multicast switches (MCSs) [2,6,8]. However, recently, WSSs are also being considered for building these A/D structures since the use of an array of optical amplifiers (OAs), to compensate the high insertion losses (ILs) inside the MCSs when large A/D structures are needed, is avoided [7,9]. Furthermore, this solution has wavelength selection capability due to the WSS nature, which is not present in MCSs, and so larger networking functionalities are expected to be provided with this solution [7].

Clearly, as the optical network evolves, the ROADM degree, *i.e.*, the number of input/output directions in a ROADM node, as well as the number of ROADMs that a signal goes through in a light-path will need to increase. In this scenario, the impact of the physical layer impairments (PLIs) inside these ROADM nodes, such as signal optical filtering, insertion losses, amplified spontaneous emission (ASE) noise and in-band crosstalk, will potentially limit both the ROADM degree, as well as, the number of cascaded ROADMs. Note that, these PLIs are cumulative along the light-path and are tightly bounded to the ROADM architecture and A/D structures.

In this work, we investigate, through Monte-Carlo (MC) simulation, the impact of the PLIs - optical filtering, ASE noise, in-band crosstalk, as well as nonlinear interference (NLI) noise caused by the Kerr effect, in a multi-degree CDC ROADM-based optical network considering 28 GBaud polarization division multiplexing (PDM) quadrature phase-shift keying (QPSK) and PDM 16 quadrature amplitude modulation (QAM) signals with Nyquist pulse shaping for 37.5 GHz channel spacing. This channel width, despite increasing spectral efficiency, is expected to increase the impact of the PLIs, limiting its usage to shorter WDM transmissions, like metro

network scenarios [10,11]. Detailed models of the R&S and B&S ROADM architectures and of the CDC A/D structures based on both MCSs and WSSs are considered in this work. With this more accurate modelling, the influence of the ROADM architecture and A/D structures on the system performance degradation induced by these PLIs is evaluated. The maximum number of cascaded CDC ROADMs that can be achieved in each ROADM configuration is also assessed. From the results extracted from our analysis, CDC ROADM design tradeoffs are also provided and discussed in this work. We would like to note that MC simulation, the method that we choose to obtain our results, is a method commonly used to study the performance of ROADM-based optical networks, e.g. [12,15,18,20], since it allows to study in a controlled environment the influence of each one of the PLIs in each of the ROADM-based scenarios considered.

The remainder of this paper is organized as follows. Section 2 discusses the related works previously published in the area of ROADM architectures and the effect of the PLIs on the network performance. Section 3 presents the CDC ROADM-based optical network model, detailing the models of both B&S and R&S architectures and also the A/D structure models based on both MCSs and WSSs. Some of the details of the MC simulator, that include the simulation of the PLIs, are also described in this section. In Section 4, some design project considerations that are typically used in today's optical networks are identified to set the simulation parameters used to assess the PLIs effect in each CDC ROADM configuration. In Section 5, the impact of ASE noise, optical filtering, in-band crosstalk and NLI noise in a CDC ROADM cascade is assessed by MC simulation and discussed. The maximum number of cascaded CDC ROADMs is also assessed for the various scenarios of ROADM architectures, degrees and A/D structures studied. Finally, the conclusions of this work are drawn in Section 6.

2. Related Work

In the literature, there have been several studies along the past several years that evaluate the impact of the referred PLIs, i.e. ASE noise accumulation, in-band crosstalk, filtering effects and fiber nonlinear effects, in some specific ROADM-based network scenarios, [12-21].

In [12-15], the impact of optical filtering and ASE noise in a cascade of ROADMs is assessed for several channel widths, e.g. 37.5 GHz, 50 GHz and 75 GHz, and WSS shapes. However, simplified models for the ROADM architectures and A/D structures have been considered and the in-band crosstalk impact has not been analyzed. For example, in [12], the impact of optical filtering is assessed considering, both, B&S and R&S architectures with a colorless and directionless A/D stage based on WSSs and QPSK and 16QAM signals with 28 and 32.5 GBaud, considering both 37.5 and 50 GHz channels. In [13], the optical filtering impact is also assessed in a similar scenario to [12], and several solutions based on optical pulse shaping to mitigate its impact are explored. Also, in [14], the optical filtering impact is assessed in a similar scenario to [12], but special attention is given to 37.5 GHz channels, as in this scenario, the optical filtering impact is a much more limiting factor than in the 50 GHz channel scenario. In the referred work, the authors study the influence of several design parameters, such as the WSS shape and the signal roll-off factor, in the optical filtering impact. In a recent work, [15], the impact of optical filtering on a R&S ROADM-based network is assessed considering QPSK, 8QAM, 16QAM, and 32 QAM modulation formats signals with symbol rates faster than 60 GBaud transported on 75 GHz channels.

In [16-21], the in-band crosstalk effect in a cascade of ROADMs is also studied in the performance analysis, alongside the filtering effects and ASE noise, and various channels widths

and WSS shapes are analyzed, as well as some specific ROADM architectures scenarios. In [16], the impact of both filtering and crosstalk is assessed considering a cascade of WSSs with different filter shapes, and 28 GBaud QPSK signals transported in 50 GHz channels. In [17], a comparison of two WSS filter shape models is performed. In particular, an analytical model and a super Gaussian-based model to fit the passband and stopband shapes of a WSS are compared. The resulting filter shapes are used to study filtering and crosstalk transmission impairments in a 34 GBaud 8QAM system for 50 GHz channels. In [18], the optical filtering and the in-band crosstalk impairments in 37.5 GHz optical channels have been evaluated, for both ROADM architectures, B&S and R&S with a colorless A/D structure. In [19], a similar performance analysis to [18] is performed, but in this work, the influence of a frequency offset between the signal and crosstalk is also analyzed. In [20], a model for a B&S ROADM architecture with a colorless A/D structure is proposed and the impact of optical filtering, ASE noise and in-band crosstalk are studied in a cascade of ROADMs for a super channel scenario, considering 16QAM signals with 32 GBaud in 50 GHz channels. The nonlinear cross phase modulation effect is also assessed in [20].

From all the above mentioned works [12-20], and to the authors' understanding, the aforementioned PLIs, ASE noise, filtering effects and in-band crosstalk, have not been evaluated thoroughly and comparatively in network scenarios with several ROADMs architectures (B&S and R&S) and A/D structures (MCS and WSS-based) combinations for the 37.5 GHz channel scenario. Moreover, the referred studies [12-20] have not considered CDC ROADMs, only colorless or colorless and directionless ROADMs have been analyzed. Recently, in [21], we have performed an analysis of CDC ROADM-based networks, but only for the 50 GHz channel scenario and considering some simplifications in the A/D structures. For example, physical limitations in MCSs with larger dimensions than the maximum commercially available (8×16), which must be built by cascading smaller MCSs, have not been considered.

3. CDC ROADM-based Optical Network Model

In this section, we present the model adopted to study the impact of the PLIs in a CDC ROADM-based optical network. We will begin by briefly explaining the function of the main building blocks of a ROADM based on a B&S and R&S architecture, followed by a description of the MCS and WSS A/D structures. Then, a short explanation of our MC simulator is provided, focusing on the origin of the PLIs.

Before going into the details of the ROADM building blocks, we will give first an example of an optical network in which several ROADM nodes with different degrees (directions) coexist. An example of a typical mesh optical network based on multi-degree ROADM nodes is represented in Fig. 1 (a). The red path in Fig. 1 (a) represents a possible light-path, established between two clients (e.g. IP clients), in the optical network. As can be observed, the optical signal has to go through several ROADMs, with possibly different degrees, before reaching its destination. The first ROADM in a given light-path is called the add ROADM (see Fig. 1 (b)), where the client signal enters the optical network and the last one is called the drop ROADM, where the optical signal reaches its destination. Between the add and drop ROADMs, there are several ROADMs called express ROADMs, where the optical signal is routed in the optical domain based on its wavelength. In a metro network, a typical link (between two ROADMs) has two OAs, one at the ROADM input and another at the ROADM output, whereas in a long-haul network, a typical link can have several OAs depending on the link length [22]. In a metro

network scenario, the OA at the ROADM input compensates the optical fiber losses, while the OA at the ROADM output compensates the insertion losses (ILs) inside the ROADM, which depend on the signal path inside the ROADM node, degree and architecture as explained in the next subsection.

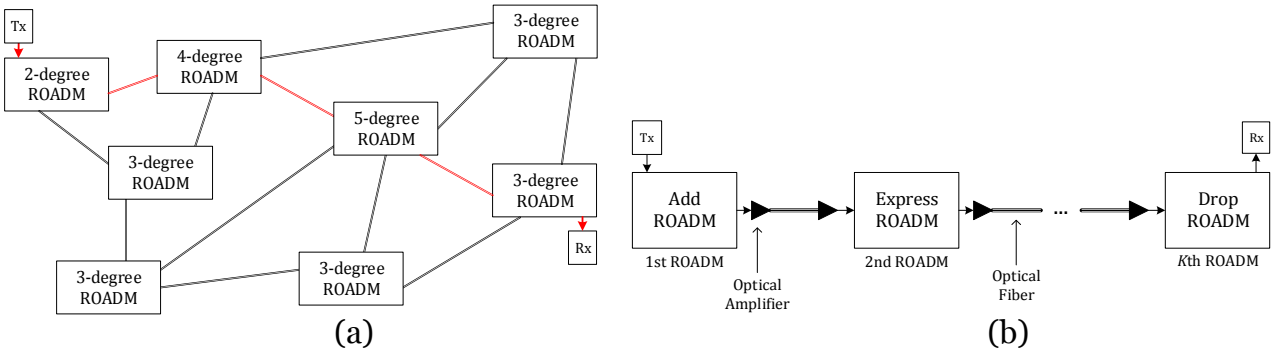

Fig. 1 - (a) ROADM-based optical network with a mesh physical topology; (b) Schematic of a light-path in a ROADM-based optical network with K ROADMs.

3.1. CDC ROADM Building Blocks

A ROADM node has two main structures, the so-called ROADM architecture, responsible for routing the optical signals, and the A/D stage responsible for adding and dropping the client signals into the optical network. These two main structures are explained next. An R-degree CDC ROADM node is schematically represented in Fig. 2. The two most used ROADM architectures are the B&S and R&S architectures. In ROADM nodes based on a B&S architecture, Component A in Fig. 2 is an optical splitter, whereas in a R&S architecture, Component A is a WSS. Component B is, in both architectures, a WSS known as the select WSS.

Regarding the A/D stage, nowadays, the most used structure for CDC ROADMs is the $N\times M$ MCSs [6]. Note that in Fig. 2, the A/D stage is assumed to have an $N\times M_t$ dimension, where N is equal to the ROADM degree and M_t is the total number of transponders of the whole A/D stage. Typically, this stage is implemented with multiple A/D structures with lower dimensions defined in this work as $N\times M$. When the dimension of the MCS structures increases, an array of OAs must be introduced in order to compensate the ILs of this structure, which increases the cost of these ROADMs. In order to avoid these arrays of OAs, an alternative A/D structure based on WSSs, the $N\times M$ WSS, is being currently investigated [7,9].

Figure 3 depicts the schematic model of a CDC ROADM drop section based on $N\times M$ MCS (Fig. 3 (a)) and $N\times M$ WSS (Fig. 3 (b)). As can be observed from Fig. 3 (a), the $N\times M$ MCS is based on $1\times M$ optical splitters and $N\times 1$ optical switches, and an array of OAs at the MCSs inputs/outputs is implemented to compensate the higher ILs introduced by the optical splitters. In Fig. 3 (b), the $N\times M$ WSS is based on $1\times M$ WSSs and $N\times 1$ optical switches. As such, A/D structures based on WSSs have wavelength selection capability, while MCS-based A/D structures do not have. The schematic model for the add structures is the same as the one shown in Fig. 3, by just having in mind the direction of the data flow, when a signal is added to the network.

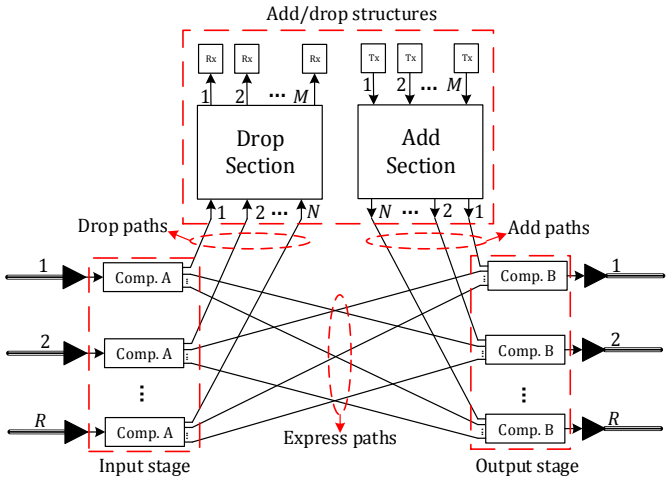

Fig. 2 - General scheme of an R-degree CDC ROADM node.

Currently one of the main issues about these A/D structures is their dimension, since the most common commercially available dimension for the MCSs is 8×16 [23] and for the WSSs is 8×24 [9,23]. In this way, due to the high number of wavelengths that are usually added/dropped in a ROADM node, the A/D stages are typically implemented with multiple A/D structures (or cards) instead of a single A/D structure [7]. In order to get a clear view of this problem, we have computed in Table I, the minimum dimension of the $N{\times}M_t$ A/D stages using a single structure as a function of the ROADM degree for 100% and a typical 20% A/D ratios [24], considering a full C-band scenario with 128 channels of 37.5 GHz [11]. The A/D ratio is the fraction of the total number of wavelengths that can be dropped/added in a ROADM, so the number of wavelengths considered for a 100% and 20% A/D ratio is, respectively, 128 and 25. The value N of the $N{\times}M_t$ A/D stage depends on the ROADM degree R, whereas, the value M_t is associated with the number of transponders in the whole A/D stage and is defined as $M_t = R \times A/D\ ratio \times 128$. For example, for an 8-degree ROADM with an A/D ratio of 20%, we need an A/D stage with a dimension of 8×205, which can be only built with multiple A/D cards. Considering the current dimension available with 8×16 MCSs, we need 13 A/D cards to achieve such dimension. Likewise, with 8×24 WSSs, the number of A/D cards needed is 9. Table II shows the necessary number of A/D cards as a function of the ROADM degree, considering A/D ratios of 20% and 100%, and both 8×16 MCS and 8×24 WSS A/D structures.

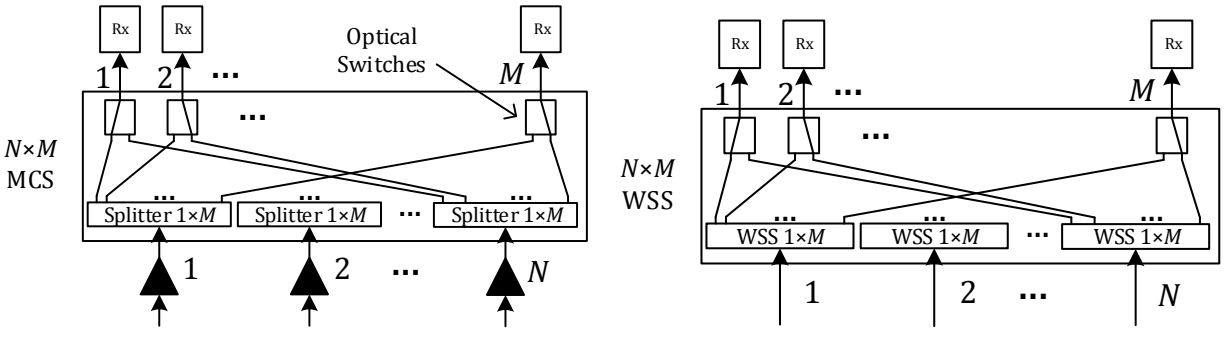

Fig. 3 - Drop structures of a CDC ROADM based on $N{\times}M$ (a) MCSs or (b) WSSs.

As already stated, one of the problems with MCS-based A/D structures is the requirement of an array of OAs inside the ROADM when the MCS dimension increases. This problem is even more serious when multiple cards are needed, since we will need parallel arrays of OAs, one array for each A/D card, increasing the A/D stage implementation cost. Hence, the number of required OAs is directly proportional to the number of cards needed by the ROADM degree *R*.

Considering the example given above, for an 8-degree ROADM with a 20% A/D ratio, we need 104 OAs. Besides the increased number of OAs, when a higher number of A/D cards is required, the dimension of the ROADM components at the input and output of the ROADM (components A and B in Fig. 2), given by 1×*X*, where *X* = (*R*-1) + number of A/D cards, must be also increased and may not be commercially available. For example, if only a single 8×205 card could be used, we will need 1×8 splitters or a 1×8 WSSs, for the B&S and R&S architectures, respectively. However, if 13 cards are used, we will need a 1×20 splitter or a 1×20 WSS instead. Nowadays, 1×35 WSSs and 1×12 splitters/couplers are commercially available [23]. Moreover, if a B&S architecture is used, the larger the optical splitter dimension at the ROADM input, the higher the ILs introduced by this component, and consequently, the OA gain at the ROADM output must be increased to compensate for this ILs. We will further discuss this issue in Section 4.

Table I

Dimension of the A/D stage as a function of the ROADM degree for both 100% and 20% A/D ratios.

	A/D ratio	
ROADM degree	100%	20%
2	2×256	2×52
4	4×512	4×103
8	8×1024	8×205

Table II

Number of A/D cards as a function of the ROADM degree for both 100% and 20% A/D ratios and for MCS and WSS-based A/D structures.

	A/D ratio			
	100%		20%	
ROADM degree	8×16 MCS	8×24 WSS	8×16 MCS	8×24 WSS
2	16	11	4	3
4	32	22	7	5
8	64	43	13	9

3.2. Simulation Model

In this subsection, we explain the MC simulation model developed in this work to study the impact of several PLIs in a CDC ROADM-based network. The flow-chart depicted in Fig. 4 specifies the various functionalities of the simulator implemented with the MATLAB software [25]. One of the building blocks of the simulator is the CDC ROADM cascade (i.e. the optical network light-path), that is further detailed in Fig. 5.

In brief, the flow-chart in Fig. 4 works as follows. The first iteration of the MC simulation is used to save the reference signal (i.e. the transmitted signal), without the

addition of any statistical sample noise functions. This reference signal allows the receiver to have the knowledge of the transmitted symbols, to compute the propagation delay of the CDC ROADM cascade and also to compute the optimum sampling time from the eye pattern of the received signal. From the propagation delay knowledge, we can synchronize the received signal impaired by the PLIs, with the transmitted signal. Notice also that any waveform distortion in the received signal, for example, caused by optical filtering, is taken into account in the received eye-pattern. On the following MC iterations, the statistical sample noise functions describing the ASE noise and in-band crosstalk are added to the signal transmitted along the CDC ROADM cascade. The received signal is then compared with the reference signal to check if the received signal has errors. This process is known as direct error counting (DEC) and when a specific number of errors is achieved (500 errors in our simulations [25]), the MC simulator stops and the bit error rate (BER) is estimated.

The BER is essentially the ratio between the number of error bits and the total number of transmitted bits, and, assuming Gray mapping, is defined by,

$$BER = N_e N_{MC} N_b log_2 m \quad (1)$$

where N_e is the number of error bits, N_{MC} is the number of generated sample functions, N_b is the number of transmitted bits in one MC iteration and m is the order of the modulation format. In this work, we evaluate the system performance for a BER equal to 10^{-3}, because we are assuming that the receiver uses forward error correction (FEC) [26, 27], which is implemented in the digital signal processing (DSP) module, a crucial functionality in today's optical receivers with coherent detection.

The other metric used in this work to evaluate the performance is the OSNR penalty. It consists in measuring, both, the required OSNR at the receiver input for a specific BER (10^{-3}), considering the received signal without the impact of the PLIs and the required OSNR at the receiver input for the same specific BER (10^{-3}), but considering the received signal with the impact of the PLIs. From the difference between the required OSNRs with and without impairments, the OSNR penalty due to that physical impairment can be estimated. In this study, we will evaluate the OSNR penalty due to optical filtering and in-band crosstalk.

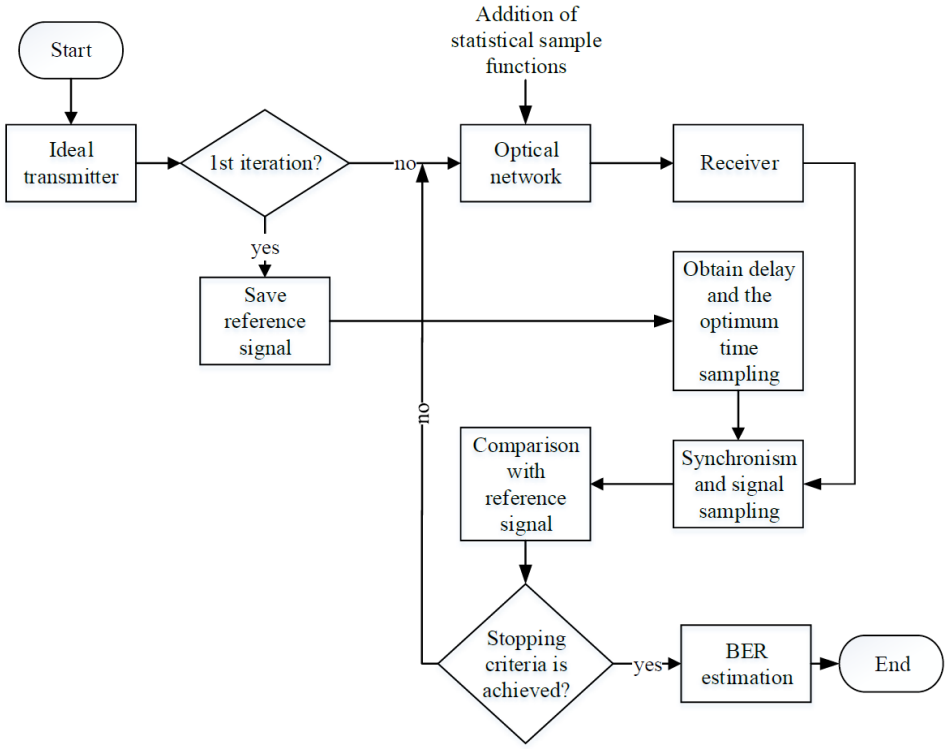

Fig. 4 – Flow-chart of the simulation model developed in this work to assess the performance of an optical signal along a CDC ROADM cascade.

In Fig. 5, the detailed schematic model of a generic cascade of K multi-degree CDC ROADMs that is referred in the simulation model flow-chart (Fig. 4) as the optical network, is presented. In Fig. 5, S_{in} represents the added input primary signal, $S_{o,K}$ the dropped output primary signal after the K^{th} ROADM and the red path represents the corresponding primary signal light-path. The in-band crosstalk signals $X_{i,(inj\ \text{or}\ addj)}$ (with $i = 1, \ldots, K$ and $j = 1, \ldots, R$) from the other ROADM directions (*in*) and from the A/D structures (*add*) and the ASE noise generated at the OAs placed at the input/output of the ROADMs are also depicted in Fig. 5. Note that to simplify Fig. 5, we only depicted one output ROADM direction corresponding to the one used by the primary signal.

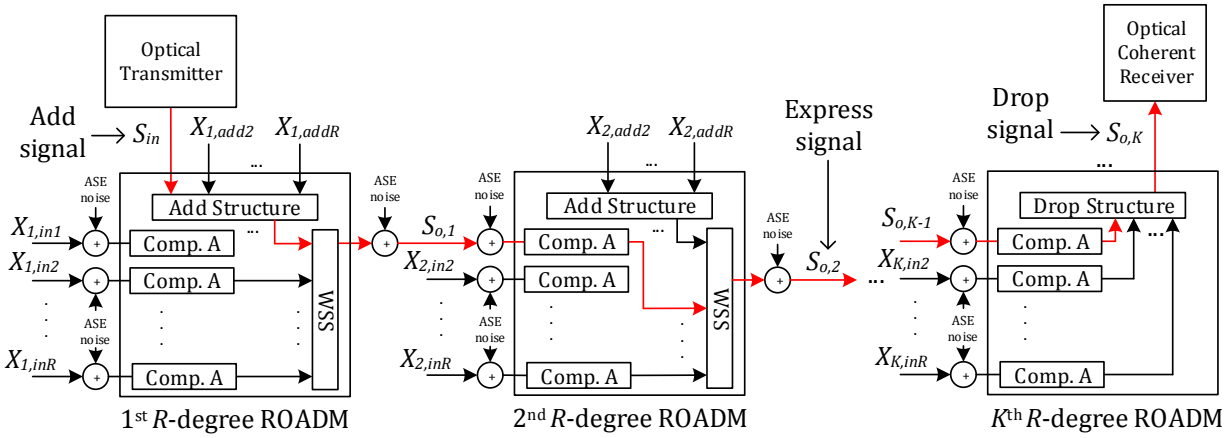

Fig. 5 - Schematic model of a cascade of K multi-degree CDC ROADM with in-band crosstalk signals and ASE noise addition.

December 5, 2020

In the simulation, at the transmitter side, where the primary signal is added to the optical network, an ideal transmitter with external modulation capable of generating 112 Gbps PDM QPSK and 224 Gbps PDM 16QAM signals with a root raised cosine (RRC) Nyquist pulse shape with a roll-off of 0.1 is considered. Note that, these bit rates correspond to a symbol rate of 28 Gbaud, when assuming a hard decision FEC with 12% overhead at the receiver DSP block [12]. Likewise, when the primary signal is dropped, an ideal optical coherent receiver modelled as in [28], is assumed.

For simulating such signals, we start by generating a sequence of bits of length 2^{13} corresponding to the information carried by the *M*-QAM primary signal using deBruijn sequences. This sequence of bits is mapped to QAM symbols with Gray coding and then, the sequence of symbols is discretized with 32 samples per symbol.

3.3. ROADM Physical Layer Impairments

In this subsection, we will briefly describe the generation of the in-band crosstalk signals, ASE noise, the optical filtering effects along the CDC ROADM cascade and fiber non-linearities using the well-known and confirmed NLI Gaussian noise model [29]. Moreover, we also highlight how these PLIs were simulated.

3.3.1 In-Band Crosstalk Simulation

In this work, we consider a worst-case scenario where all ROADM directions are possible in-band crosstalk sources, *i.e.*, the same wavelength as the primary signal appears in all ROADM inputs and add ports. Consequently, the number of interferers depends on the ROADM degree and on the A/D ratio. This number can be computed as follows. When the signal is added in the 1st ROADM node, it is impaired by $R-1$ in-band crosstalk signals that come from the ROADM inputs and also by $R-1$ in-band crosstalk signals that come from the ROADM add section. So, the total number of in-band interferers in the 1st ROADM node is $2(R-1)$. When the signal is expressed in the ROADM node, the number of in-band interferers is $R-2$, from the ROADM inputs and more $R-2$ interferers from the add section, giving a total of $2(R-2)$ in-band interferers [30]. Note that the in-band interferers from the ROADM inputs with a R&S architecture are second order interferers, since they are blocked twice by the WSSs at the ROADM input and output. On the other hand, with a B&S ROADM architecture, the interferers are blocked only once at the ROADM output, and correspond to first order interferers. Regarding the in-band interferers from the added signals, they are blocked twice in the B&S architecture (one in MCS A/D structure and another one at the ROADM output) and blocked three times in the R&S architecture (two times in WSS-based A/D structure and one time at the ROADM output). When the signal is dropped, only $R-1$ in-band interferers from the ROADM inputs appear.

In our MC simulator, the crosstalk is generated considering that the interfering signals have the same attributes of the primary signal (i.e. modulation format and bit rate), but the bits of each interfering signal are generated randomly in each MC simulation iteration. Hence, they are statistically independent of the primary signal, and have a random phase difference and a time misalignment in relation to the primary signal. The time misalignment is modelled as a uniformly distributed random variable between zero and the symbol period, and the phase difference has also a uniform distribution within the interval $[0,2\pi[$ [30]. In each iteration of the

MC simulation, a sample function of each one of the interfering signals $X_{i,(inj \text{ or } addj)}$ shown in Fig. 5 is generated, similarly to what is done in [25].

3.3.2 ASE Noise Simulation

In this work, we consider that the OAs are erbium doped fiber amplifiers (EDFAs) and the generated ASE noise is modelled by a zero mean white stationary Gaussian process characterized by the respective power spectral density [25]. Since, in our work, we have OA gains that can range between 5 and 25 dB (see Section 4), we consider a 7 dB noise figure for a 15 dB or smaller OA gain and a 5 dB noise figure for a 25 dB or higher OA gain. For OA gains between 15 and 25 dB, a simplified model based on a linear interpolation is used to estimate the noise figure [31].

In our MC simulator, the ASE noise is generated considering that in each iteration of the simulator, an ASE noise sample function is generated by each one of the OAs considered in Fig. 5, so a realistic lumped amplification scenario is used. Note that in this figure, the ASE noise addition in MCSs-based A/D structures is not shown, since we consider the array of OAs that originates these ASE noise terms as part of the A/D structure.

3.3.3 Filtering Effects Simulation

Next, we describe the models used in the simulation to characterize the different ROADM components. In particular, each component of the ROADM must be modelled by its transfer function, which characterizes both the amplitude and phase response of that component. In what concerns the WSS (based on LCoS technology) model, we used super Gaussian optical filters with low pass equivalent amplitude transfer functions given by (2) for the passband filter [12] and by (3) for the stopband filter,

$$\boldsymbol{H_p(f)} = \boldsymbol{e}^{-\left[\left(\frac{f}{B_0/2}\right)^{2n}\frac{ln2}{2}\right]} \tag{2}$$

$$\boldsymbol{H_b(f)} = \boldsymbol{(1-a).e}^{-\left[\left(\frac{f}{B_0/2}\right)^{2n}\frac{ln2}{2}\right]} \tag{3}$$

where n is the super Gaussian filter order, B_o is the −3 dB bandwidth of the optical filter and a is the blocking amplitude of the stopband filter in linear units. The super Gaussian model has been shown to characterize accurately experimental transfer functions [12] by properly setting n and B_o. Figure 6 depicts the amplitude transfer functions of the passband filters (Fig. 6 (a)) and stopband filters (Fig. 6 (b)) for the 50 GHz (solid lines) and 37.5 GHz (dashed lines) channels. The amplitude transfer function for 50 GHz channels is shown only for comparison with the one for the 37.5 GHz channels. In this work, we considered that all filters are aligned with the central frequency of the primary signal, which is considered as an optimistic scenario, since due to fabrication issues, ageing, and temperature variations, in practice, there is a slight misalignment between those frequencies. The super Gaussian filter orders n are 5.5 and 4.2 and the −3 dB bandwidth B_o is equal to 46.4 GHz and 35.2 GHz, respectively, for 50 GHz and 37.5 GHz channels [12], and the blocking amplitude (i.e. isolation level) for the stopband filter is considered to have a typical value of −40 dB [12]. Thus, the WSSs are the ROADM components

responsible for the optical filtering of the primary signal, in-band crosstalk and ASE noise. The optical filtering is seen as an important PLI, particularly in a cascade of ROADMs where the passband narrowing limits the transmission distance [12], [16]. Regarding the WSSs ILs, we considered that both 1×*N* and *N*×*M* WSSs have the same ILs of 7 dB, a typical value found in the literature [5], [9].

Regarding the modelling of the optical splitters/couplers, since they have no frequency selective capability, they are characterized only by their ILs. The ILs introduced by these components are computed by $10\log_{10} X + A_{exc}$, where X is the number of outputs/inputs and A_{exc} are the excess losses. A typical value of 4, 7, 11, 15 and 19 dB is considered, respectively for the ILs of 1×2, 1×4, 1×8, 1×16 and 1×32 splitters [32]. For the X×1 optical switches, inside the MCS and WSS A/D structure (see Fig. 3), we considered a typical IL of 1 dB and a blocking extinction of about 60 dB.

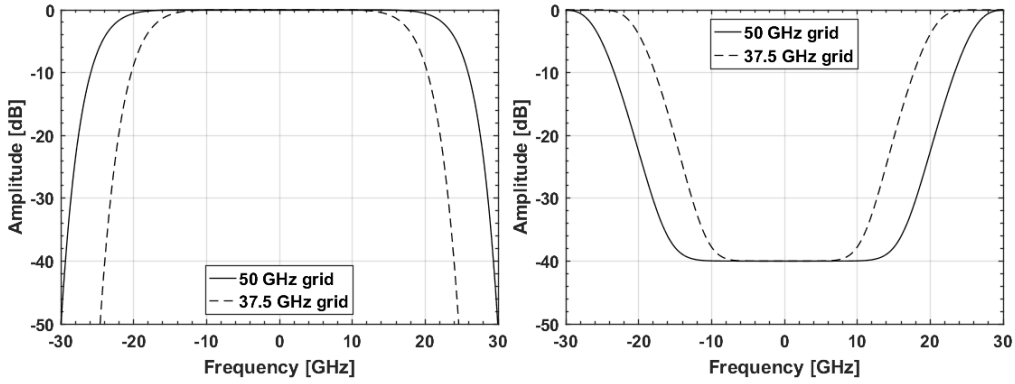

Fig. 6 - WSS transfer functions for the (a) passband and (b) stopband filters for the 50 GHz (solid lines) and 37.5 GHz (dashed lines) channels.

3.3.4 Fiber Non-linearities Simulation

The fiber non-linearities in an uncompensated coherent optical communication system can be characterized as NLI noise, when its effect on the performance is "mild" [29], [33]. The impact of NLI noise manifests itself as an additive Gaussian noise (GN) at the end of the optical path, being characterized by the model known as the GN model [29]. In this model, it is assumed that the NLI can be modeled as an additive GN statistically independent of the signal and ASE noise generated in EDFAs and also that it accumulates incoherently along the transmission path. Hence, the NLI noise can be taken into account in the OSNR, simply by adding the NLI noise power to the accumulated ASE noise power at the optical receiver input. Although simple, this model has proven to provide reliable results of the effect of fiber non-linearities in the performance of coherent optical communication links [33], and is typically applied to optical network performance studies [31], [34].

In this work, the NLI noise power at the input of the optical coherent receiver is estimated using the asymptotic approach presented in [35]. In presence of ASE and NLI noise, the OSNR at the optical receiver input is maximized when the power of the accumulated ASE noise is twice the NLI noise power [29], being this maximum OSNR obtained for a specific transmitted signal power. Hence, in all results presented in this work, the power of the signal launched at the optical fiber input is optimized to maximize

the received OSNR, for each specific system configuration depending on: the modulation format, QPSK or 16QAM, the ROADM architecture, B&S or R&S, the A/D structure, MCSs or WSSs, and also as a function of the ROADM degree.

4. CDC ROADM-based Optical Network Design Project Considerations

In this section, we consider some design project considerations that are typically used in today's optical networks. These design considerations will allow us to identify the maximum degree of a CDC ROADM that can be used for optical networks operating with 37.5GHz-spaced 28 Gbaud channels, considering B&S or R&S architectures with both A/D structures, MCSs or WSSs-based. These findings will be used in Section 5, where the impact of the PLIs in a CDC ROADM-based optical network is assessed through MC simulation. We would like to highlight that the B&S architecture with MCS-based A/D structures is not used in practice, however it is analyzed in this work for comparison purposes with the other studied architectures. The reason why it is not used is that, in the drop side, each coherent receiver would see all WDM channels from the input WDM port where the detected channel is dropped. This would saturate the total input power seen by the receiver and then yield a substantial detection penalty.

The first design consideration comes from the fact that commercial OAs have a minimum and maximum gain that should not be exceeded. In the case of EDFAs, the minimum gain is around 5 dB and the maximum gain is around 25 dB [23]. ROADM implementations that lead to OA gains outside this range will not be considered in this work.

As referred in Section 3, the OA at the ROADM input compensates the fiber losses between ROADM nodes. In this work, we consider a fiber span of 80 km between each ROADM node and a fiber attenuation coefficient of 0.25 dB/km. Consequently, the OA at ROADMs inputs will have a fixed gain of 20 dB. Regarding the OA at the ROADM output, its gain is dimensioned based on the express path losses. The express path depends on the ROADM architecture and, for ROADMs based on a B&S architecture, also depends on the ROADM degree and number of cards in the A/D structures. Besides, this is one of the main reasons why MCS-based A/D structures are not used with the B&S architecture. These two parameters will influence the dimension of the optical splitter at the ROADM input and, consequently, the express path losses. Table III shows the OA gain at the ROADM output for the B&S and R&S architectures, for several ROADM degrees considering a single card in the A/D stage. Table IV shows the OA gain at the ROADM output, but considering multiple cards in the A/D stage, and as a function of the A/D structure type and A/D ratio. From Table IV, we can conclude that, for an 100% A/D ratio, more than 25 dB gain is required at the ROADM output for 4 and 8-degree ROADMs with MCSs-based A/D structures, whereas, with WSSs-based A/D structures, only for the 8-degree scenario there is such limitation. These values are highlighted in red in Table IV.

Table III

OA gain at the ROADM output with a single A/D card.

ROADM architecture	B&S			R&S		
ROADM degree	2	4	8	2	4	8
OA gain at ROADM output [dB]	11.0	14.0	18.0	14.0		

Table IV
OA gain at the ROADM output with multiple A/D cards.

	A/D structure	8×16 MCSs						8×24 WSSs					
	ROADM architecture	B&S			R&S			B&S			R&S		
	ROADM degree	2	4	8	2	4	8	2	4	8	2	4	8
OA gain at ROADM output [dB]	100% A/D ratio	22.3	26.4	29.5	14.0			14.0	24.0	28.0	14.0		
	20% A/D ratio	15.0	19.0	23.0	14.0			14.0	18.0	22.0	14.0		

The calculation of the gain of the OAs inside the MCSs-based A/D structures is explained next. As referred in Section 3, the MCSs are composed by optical switches and optical splitters/couplers and, the ILs introduced by each MCSs are obtained by summing the ILs of the two components just mentioned. We consider that each OA in the array at the MCSs-based drop section can compensate all drop losses, i.e. the losses from the MCS and from the ROADM input component, as given by (4), until it reaches its maximum output power. In such cases, where the OA in the array is working at its maximum output power (assumed as 20 dBm), the remainder of the uncompensated drop losses is compensated by adjusting the gain inside the optical coherent receiver, e.g. [36]. Likewise, the OA gain at the MCSs-based add section is computed in order to compensate all ILs of the add path but having in mind the OA gain at ROADM output. Hence, to the required gain for the MCSs-based add section, the losses of the component at ROADM input (Comp. A) are subtracted, as given by (5)

$$G_{MCS\_DROP}\,[dB] = ILs_{Comp.A} + ILs_{MCS} = ILs_{Comp.A} + 10\log_{10} M + A_{exc} + 1 \quad (4)$$

$$G_{MCS\_ADD}\,[dB] = ILs_{MCS} - ILs_{Comp.A} = 10\log_{10} M + A_{exc} + 1 - ILs_{Comp.A} \quad (5)$$

where ILs_{CompA} are the insertion losses of Component A defined in Fig. 2 and ILs_{MCS} are the insertion losses of the MCS.

The second design consideration is related with the maximum output power allowed in an EDFA to minimize fiber non-linear effects. A maximum OA output power of 22 dBm is considered [23] for the OAs at the input/output of the ROADM, which leads to a maximum power of nearly 1 dBm per channel, considering 128 wavelengths (@37.5 GHz channel spacing).

The third, and final design consideration comes from the fact that commercially available transponders with today's DSP ensure a specific target BER for a range of optical powers. We have considered that the transponder optical power range is between 0 and –15 dBm, to ensure a target BER of 10^{-3}. Consequently, in the simulator, we are assuming that the coherent receiver has the capacity of introducing gain in the optical received signal between 0 and 15 dB, if required, e.g. [36]. Note that for B&S ROADM-based optical networks with WSSs-based A/D structures, an optical coherent receiver gain higher than 15 dB is required for ROADM degrees higher than 2. Nevertheless, we do not discard these cases, because the excess of gain in the

optical coherent receiver can be reduced by increasing the OA gain at the ROADM input, which was previously set to 20 dB.

5. Impact of the Physical Layer Impairment on CDC ROADM-based Optical Networks

In this section, the impact of the ASE noise, optical filtering and in-band crosstalk in a cascade of multi-degree CDC ROADMs will be analyzed. In this analysis, we will consider ROADMs with B&S and R&S architectures and with MCSs and WSSs-based A/D structures.

The referred analysis consists on assessing the system performance by measuring the OSNR at the optical receiver input for a particular modulation format for 12.5 GHz reference bandwidth, as well as the OSNR penalties, due to optical filtering effects and in-band crosstalk. In order to estimate the BER, associated with the measured OSNR, we use in our MC simulation, as stopping criterion 500 counted errors [25]. Note, that we have obtained, by simulation and considering a back-to-back scenario, for a BER = 10^{-3}, an OSNR = 13 dB and 20 dB, respectively, for the QPSK and 16QAM modulation formats, which is in complete agreement with the values found in the literature, *e.g.* [12, 37]. The OSNR penalty due to a specific impairment (e.g. optical filtering effects) is assessed by measuring the difference between the OSNR, at the receiver input, for a target BER of 10^{-3} without the influence of that impairment and the OSNR with that impairment.

In our simulation model (see Fig. 5), we use both 112 Gbps PDM QPSK and 224 Gbps 16QAM signals shaped by an RRC Nyquist pulse with a roll-off factor of 0.1, considering 37.5 GHz channels. Moreover, the WSSs inside the ROADM have an isolation level of −40 dB and each A/D stage built with 8×16 MCS or 8×24 WSS cards has an A/D ratio of 20%. Also, a maximum of 10 cascaded nodes is assumed, as it is considered a reasonable maximum number of transit nodes in today's optical transport networks. Regarding the number of cascaded ROADMs that can be attained by a light-path, we consider that the signal is added at the first ROADM of the cascade and dropped at the last ROADM. This means that, for example, for a cascade of 6 ROADMs, the signal under study is considered to be dropped at the 6th ROADM.

At the end of this section, we will summarize the tradeoffs between the studied ROADM architectures and A/D structures in terms of the PLIs impact.

As a final remark, we would like to mention that we have obtained the results presented in [12] with our simulator, for both QPSK and 16QAM modulation formats and both 37.5 GHz and 50 GHz channels. Only the ASE noise and filtering penalties have been assessed in [12], by loading the ASE noise at the end of the optical network, instead of distributing the ASE noise through lumped amplification along the network as we do throughout this work. Furthermore, to obtain the results in [12], we considered a R&S ROADM architecture with a colorless and directionless A/D structure, instead of the CDC structure analyzed in this work.

5.1. Optical Filtering Impact

In this subsection, to assess the optical filtering impact in the CDC ROADM-based optical network performance, we use the simulation model shown in Fig. 5, considering the optical filtering of the signal in the primary light-path, the addition and filtering of the ASE noise in the primary signal light-path and neglecting the in-band crosstalk interferers. Notice that the impact of the optical filtering does not depend on the ROADM degree, and only depends on the number

of cascaded ROADMs in the signal light-path and on the A/D structures type. Hence, to obtain the results shown in this subsection, in the simulation, we have used only 2-degree ROADMs to assess the optical filtering impact. Figure 7 depicts the OSNR penalty as a function of the CDC ROADMs nodes number with A/D structures based on 8×16 MCSs cards (Fig. 7 (a)) and on 8×24 WSSs cards (Fig. 7 (b)), for both B&S (lines with circles) and R&S (lines with crosses) ROADM architectures and for the QPSK (solid lines) and 16QAM (dashed lines) modulation formats. We evaluate the impact of optical filtering by assessing its impact on the OSNR penalty. First, we estimate the required OSNR to achieve the target BER for the reference scenario with two nodes, $OSNR_{2nodes}$. Then, we calculate the OSNR to achieve the same BER with the increasing number of ROADM nodes, $OSNR_{Xnodes}$. The OSNR penalty due to optical filtering, calculated in relation to the two ROADMs reference scenario, is the subtraction of these two OSNRs, $\Delta OSNR = OSNR_{Xnodes} - OSNR_{2nodes}$.

As expected, the optical filtering impact is more significant for the 16QAM format, as we can observe in Fig. 7, by comparing the dashed and the solid lines, and has also shown in [12], [31]. For example, for B&S ROADM architecture and MCSs-based A/D structures (lines with crosses in Fig. 7 (a)), the OSNR penalty due to the optical filtering at the end of 10 cascaded CDC ROADMs is 0.3 dB and 1.9 dB for the QPSK and 16QAM modulation formats, respectively. These OSNR penalties are in a very good agreement with the results presented Fig. 1d) and f) of [12], when "sharp" optical filtering is used throughout the cascade. This good agreement indicates that our simulator is taking into account the effect of optical filtering properly. Comparing Fig. 7 a) with Fig. 7 b), we can conclude that, the WSSs-based A/D structures lead to a higher OSNR degradation due to the optical filtering. This is due to the extra filtering stage that the signal suffers in the A/D structures based on WSSs. Considering the R&S ROADM architecture, the OSNR penalty due to the optical filtering is higher than for the B&S ROADMs, due to the double filtering stage that the signals suffer at the ROADMs input and output. For example, for 16QAM and WSSs-based A/D structures, the OSNR penalty at the end of 6 cascaded ROADMs is 1.1 dB and 3.8 dB for the B&S and R&S architectures, respectively. Note that, for the 16QAM format and the R&S ROADMs architecture, there is a major limitation in terms of the OSNR penalty due to the optical filtering, limiting the number of cascaded CDC ROADMs to around 6, as seen in Fig. 7 (b).

Regarding the impact of the filtering solely on the ASE noise, in the primary signal light-path, it has been confirmed by simulation that it does not have a significant impact in the CDC ROADM-based optical network performance degradation.

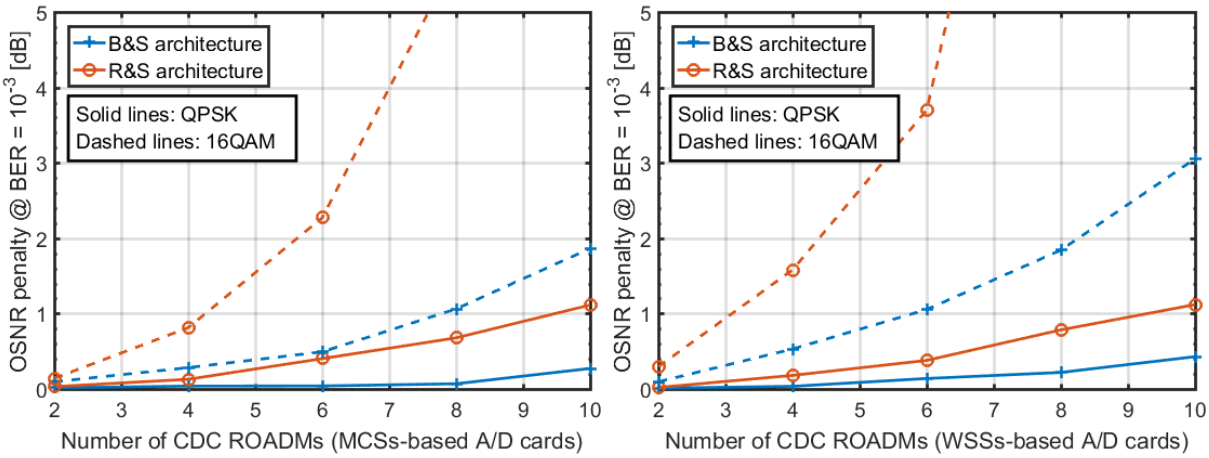

(a) (b)

Fig. 7 - OSNR penalty due to the optical filtering as a function of the number of CDC ROADMs with (a) 8×16 MCSs and (b) 8×24 WSSs-based A/D cards for the QPSK (solid lines) and 16QAM (dashed lines) modulation formats, both ROADM architectures, B&S (blue lines) and R&S (red lines).

5.2. In-Band Crosstalk Impact

In this subsection, we investigate the in-band crosstalk impact on the network performance. We use the network model of Fig. 5, considering ASE noise and in-band crosstalk that come from either the ROADMs inputs and ROADMs add sections, and the optical filtering effect from the several WSSs.

Figures 8 and Fig. 9 depict the OSNR penalty due to the in-band crosstalk as a function of the number of the CDC ROADMs for several ROADM degrees, considering B&S and R&S ROADM architectures with both A/D structures, MCSs and WSSs-based structures. Figure 8 shows the simulation results for the QPSK modulation format, while Fig. 9 refers to the 16QAM format. The simulations results shown in Fig. 8 and Fig. 9 confirm that, the QPSK modulation format is more tolerant to in-band crosstalk than the 16QAM format, as expected and already shown in [37].

By comparing the ROADM architectures, we can observe a higher in-band crosstalk tolerance with the R&S architecture. In this case, the in-band crosstalk interferers from the ROADM inputs pass through more blocking filters than for the B&S architecture, which consequently leads to a lower OSNR penalty degradation due to this impairment using the R&S architecture. For the QPSK modulation format, the OSNR penalties due to the in-band crosstalk obtained with the R&S architecture are practically negligible, lower than 0.5 dB at the end of 10 cascaded CDC ROADMs. This observation is also valid for the 16QAM format with ROADMs using WSSs-based A/D structures. For the 16QAM format with R&S architecture and MCSs-based A/D structures, the OSNR penalty is about 2 dB after eight cascaded 8-degree ROADMs. We can also observe in Fig. 8 (a) (ROADMs with MCSs-based A/D structures and QPSK modulation format) that the OSNR penalty is almost constant along the ROADM cascade with B&S architecture. The reason for this behavior is the extremely high ASE noise power generated by the OAs along the light-path in this case, that masks the in-band crosstalk power, leading to very low OSNR penalties due to in-band crosstalk along the ROADM cascade. As the OSNR is lower with WSS-based A/D structures than with MCSs, for both ROADM architectures, we

observe higher OSNR penalties due to in-band crosstalk for a higher number of cascaded ROADMs with WSSs than with MCSs-based A/D structures.

Finally, Figs. 8 and 9 show also that the impact of in-band crosstalk is highly dependent on the ROADM degree for the B&S architecture, and that the in-band crosstalk penalty is much more severe for the MCSs-based A/D structures than for WSSs ones, when the number of cascaded nodes is low. For a higher number of cascaded ROADMs, the in-band crosstalk penalty in ROADMs with WSS-based A/D structures becomes comparable or even higher than the penalty found with MCSs-based structures.

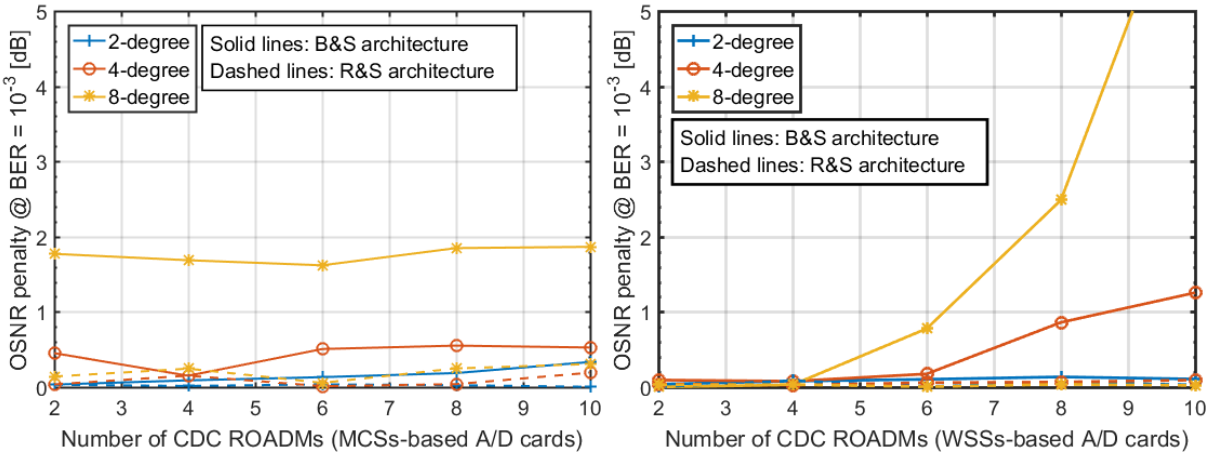

(a) (b)

Fig. 8 - OSNR penalty due to the in-band crosstalk as a function of the number of CDC ROADMs with (a) 8×16 MCSs and (b) 8×24 WSSs-based A/D cards, for QPSK format, several ROADM degrees and both B&S (solid lines) and R&S (dashed lines) ROADM architectures.

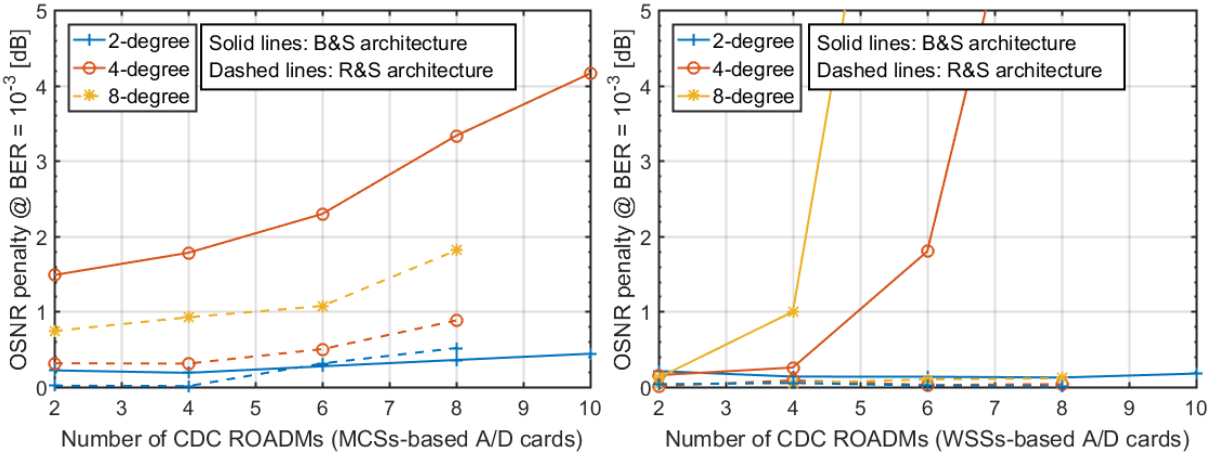

(a) (b)

Fig. 9 - OSNR penalty due to the in-band crosstalk as a function of the number of CDC ROADMs with (a) 8×16 MCSs and (b) 8×24 WSSs-based A/D cards, for 16QAM format, several ROADM degrees and both B&S (solid lines) and R&S (dashed lines) ROADM architectures.

5.3. ROADM Design Tradeoffs

After assessing the impact of the PLIs, in particular optical filtering and in-band crosstalk, in a cascade of CDC ROADMs considering the B&S and R&S architectures with both MCSs and WSSs-based A/D structures, we use this subsection to summarize our results and established some ROADM design tradeoffs that can be useful in the design of an optical network operating with 37.5 GHz-spaced 28 Gbaud channels. In particular, we are going to assess the maximum number of cascaded ROADMs for each one of the four studied scenarios taking into account the impact of the PLIs analyzed so far in this work., i.e. ASE noise accumulation, optical filtering effects, and in-band crosstalk. Moreover, in this sub-section, we will also take into account the degradation induced by the impact of the NLI due to Kerr effect in the optical fiber as described in subsection 3.3.4. In this work, to estimate the NLI contribution, we consider a fiber dispersion parameter of 16 ps/(nm·km) and a non-linearity coefficient of 1.3 $W^{-1}{\cdot}km^{-1}$.

In order to assess the maximum number of cascaded ROADMs, and considering that current commercial-grade transponders can deliver up to 0 dBm output power for the channel outgoing from their transmitter part, we have optimized that power with respect to NLI to maximize the OSNR at the receiver input [29]. The results obtained for the four scenarios are shown in Table V and the corresponding comments and conclusions are as follows:

- Scenario 1: B&S architecture with MCS-based A/D structure – this scenario is the most restrictive in terms of the ROADM degree for both modulation formats. Furthermore, as already mentioned, it is a combination that is not used in practice;
- Scenario 2: B&S architecture with WSS-based A/D structure - this scenario is clearly less limitative in terms of reach and ROADM degree than Scenario 1. For 4 and 8-degree ROADMs, we can see that the number of cascaded ROADMs is more than the double comparing to Scenario 1;
- Scenario 3: R&S architecture with MCS-based A/D structure – this is the scenario where it is possible, for QPSK signals, to have ROADM degrees as large as 8 and longer cascades with 13 ROADMs. For 16QAM signals, cascades with 3 ROADMs are allowed for all the degrees considered;
- Scenario 4: R&S architecture with WSS-based A/D structure – this scenario has a similar performance to Scenario 3 in terms of ROADM degree and number of cascaded ROADMs for both modulation formats. We also observe that for WSS A/D structures and 16QAM signals, the number of cascaded ROADMs is similar for both R&S and B&S architectures.

As a final remark, we note that several techniques can be used to mitigate these PLIs, such as the use of low noise OAs, digital signal processing techniques to mitigate the optical filtering impact [13], or even WSSs with higher isolation levels.

Table V
Maximum number of cascaded ROADMs for the four scenarios.

		QPSK		16QAM	
	ROADM degree	B&S	R&S	B&S	R&S
MCSs	2	17	13	3	3
	4	4	13	1	3
	8	3	13	-	3
WSSs	2	18	14	5	4
	4	11	14	4	4
	8	8	14	3	4

6. Conclusions

In this work, we have assessed the PLIs impact on the performance of optical networks based on multi-degree CDC ROADMs considering Nyquist pulse shaped QPSK and 16QAM signals in 37.5 GHz width channels. We have considered four ROADMs configurations: B&S and R&S architectures with MCSs or WSSs-based A/D structures. The PLIs analyzed along this work were the ASE noise, optical filtering, in-band crosstalk and NLI.

Firstly, we have studied the impact of the optical filtering on the ROADMs cascade performance and have concluded that it is independent on the ROADM degree. The degradation due to optical filtering is more relevant for R&S ROADM architectures with WSS-based A/D structures and for 16QAM signals. We also analyzed the in-band crosstalk and as expected the B&S ROADM architecture with MCS-based A/D structures is the scenario where this impairment is more significant, especially for 16QAM signals.

In summary, we have concluded that for QPSK signals, typically used in long-haul networks, R&S ROADM architectures with both MCS and WSS-based A/D structures allow larger ROADM degrees, as large as 8, and larger ROADM cascades than B&S architectures. The WSS A/D structures have an expectable larger range of networking functionalities regarding the MCS-based A/D structures, and also avoid the use of potentially large arrays of EDFAs needed in MCS structures. So then, the R&S architecture with WSS A/D structure can be seen as a potential architecture for long-haul network nodes. We have also observed that for 16QAM signals, typically used for shorter link ranges, and WSS A/D structures, the number of cascaded ROADMs is similar for both B&S and R&S architectures. Since the B&S architecture has a cost advantage regarding the R&S architecture, we foresee its use alongside WSSs-based A/D structures in metro networks.

Funding: This work was supported by Fundação para a Ciência e Tecnologia (FCT) of Portugal within the project of Instituto de Telecomunicações UID/EEA/50008/2019.

References

[1] P. Winzer and D. Neilson, "From scaling disparities to integrated parallelism: a decathlon for a decade," *J. Lightwave Technol.*, vol. 35, pp. 1099-1115, 2017.
[2] T. Zami, "Multiflow application for WDM networks with multicarrier transponders serving superchannels in contentionless OXCs [Invited]," *J. Opt. Commun. Netw.*, vol. 9, pp. A114-A124, 2017.
[3] M. Schiano, A. Percelsi, and M. Quagliotti, "Flexible node architectures for metro networks [Invited]," *J. Opt. Commun. Netw.*, vol. 7, pp. B131-B140, 2015.

[4] J. Simmons, Optical network design and planning, 2nd ed., Springer, 2014.
[5] H. Yang, B. Robertson, P. Wilkinson, and D. Chu, "Low-cost CDC ROADM architecture based on stacked wavelength selective switches," *J. Opt. Commun. Netw.*, vol. 9, pp. 375-384, 2017.
[6] W. I. Way, "Optimum architecture for M×N multicast switch-based colorless, directionless, contentionless, and flexible-grid ROADM," in *National Fiber Optic Engineers Conference (NFOEC)*, Optical Society of America, 2012, paper NW3F.5.
[7] T. Zami and B. Lavigne, "Advantages at network level of contentionless N×M adWSS," in *Optical Fiber Communication Conf. (OFC)*, 2019, paper M1A.2.
[8] Y. Ma, *et al.*, "Novel CDC ROADM architecture utilizing low loss WSS and MCS without necessity of inline amplifier and filter," in *Optical Fiber Communication Conf. (OFC)*, 2019, paper M1A.3.
[9] P. Colbourne, S. McLaughlin, C. Murley, S. Gaudet, and D. Burke, "Contentionless twin 8x24 WSS with low insertion loss," in *Optical Fiber Communication Conf. (OFC)*, 2018, paper Th4A.1.
[10] T. Zami, B. Lavigne, S. Weisser, I. Ruiz, "How efficient can routing of individual 37.5 GHz-spaced 100 Gb/s 33 GBaud carriers be in WDM mesh core networks?", in *European Conf. on Optical Communications (ECOC)*, 2018, paper Th2.59.
[11] ADVA FSP-3000 optical transport solution: http://lightriver.com/item/ adva-fsp-3000/
[12] A. Morea, *et al.*, "Throughput comparison between 50-GHz and 37.5-GHz grid transparent networks [Invited]," *J. Opt. Commun. Netw.*, vol. 7, pp. A293-A300, 2015.
[13] T. Rahman *et al.*, "On the mitigation of optical filtering penalties originating from ROADM cascade," *IEEE Photonics Technology Letters*, vol. 26, pp. 154-157, 2014.
[14] M. Filer and S. Tibuleac, "Cascaded ROADM tolerance of MQAM optical signals employing Nyquist shaping," in *IEEE Photonics Conf. (IPC)*, 2014, pp. 268-269.
[15] T. Zami, I. de Jauregui Ruiz, A. Ghazisaeidi, and B. Lavigne, "Growing impact of optical filtering in future WDM networks," in *Optical Fiber Communication Conf. (OFC)*, 2019, paper M1A.6.
[16] M. Filer and S. Tibuleac, "Generalized weighted crosstalk for DWDM systems with cascaded wavelength-selective switches," *Opt. Express*, vol. 20, pp. 17620-17631, 2012.
[17] J. Pan, C. Pulikkaseril, L. Stewart and S. Tibuleac, "Comparison of ROADM filter shape models for accurate transmission penalty assessment," in *IEEE Photonics Conf. (IPC)*, 2016, pp. 550-551.
[18] J. Pan and S. Tibuleac, "Filtering and crosstalk penalties for PDM-8QAM/16QAM super-channels in DWDM networks using broadcast-and-select and route-and-select ROADMs," in *Optical Fiber Communication Conf. (OFC)*, 2016, paper W2A.49.
[19] J. Pan and S. Tibuleac, "In-band crosstalk analysis for Nyquist PDM-16QAM in flexible grid transmission," in *IEEE Photonics Conf. (IPC)*, 2017, pp. 439-440.
[20] T. Nakagawa, Y. Mori, K. Maru, H. Matsushita and M. Jinno, "Linear and nonlinear impairments when adding and dropping superchannels in an elastic optical network," in *Asia-Pacific Conf. on Communications (APCC)*, 2015, pp. 25-28.
[21] D. Sequeira, L. Cancela and J. Rebola, "Physical layer impairments in a cascaded multi-degree CDC ROADMs with NRZ and Nyquist pulse shaped signals," in *International Joint Conf. on e-Business and Telecommunications (ICETE 2018)*, 2018, pp. 223-231.
[22] B. Clouet, R. Schimpe and A. Schex, "On the design trade-offs of ROADM architectures," in *Photonic Networks Symposium*, 2014, pp. 1-4.
[23] Lumentum: www.lumentum.com
[24] L. Zong, H. Zhao, Z. Feng, and Y. Yan, "Low-cost, degree-expandable and contention-free ROADM architecture based on M × N WSS," in *Optical Fiber Communication Conf. (OFC)*, 2016, paper M3E.3.
[25] B. Pinheiro, J. Rebola and L. Cancela, "Impact of in-band crosstalk signals with different duty-cycles in M-QAM optical coherent receivers", in *European Conf. on Network and*

Optical Communications (NOC), 2015, pp. 1-6.
[26] G. Tzimpragos, C. Kachris, I. Djordjevic, M. Cvijetic, D. Soudris, and I. Tomkos, "A Survey on FEC Codes for 100 G and Beyond Optical Networks", IEEE Communication Surveys & Tutorials, vol. 18, pp. 209-221, 2016.
[27] ITU-T G.975.1 Series G: Transmission Systems and Media, Digital Systems and Networks.
[28] M. Seimetz and C. Weinert, "Options, feasibility, and availability of 2 × 4 90° hybrids for coherent optical systems," *J. Lightwave Technol.*, vol. 24, pp. 1317-1322, 2006.
[29] P. Poggiolini, G. Bosco, A. Carena, V. Curri, Y. Jiang, and F. Forghieri, "The GN model of fiber non-linear propagation and its applications," *J. Lightwave Technol.,* vol. 32, pp. 694–721, 2014.
[30] D. Sequeira, L. Cancela and J. Rebola, "Impact of physical layer impairments on multi-Degree CDC ROADM-based optical networks," in *International Conf. on Optical Network Design and Modeling (ONDM)*, 2018, pp. 94-99.
[31] J. Pedro, "Designing transparent flexible-grid optical networks for maximum spectral efficiency", *J. Opt. Commun. Netw.*, vol. 9, pp. c35-c44, 2017.
[32] The Fiber Optic Association: https://www.thefoa.org/tech/ref/testing/test/couplers.html
[33] P. Poggiolini and Y. Jiang, "Recent Advances in the Modeling of the Impact of Nonlinear Fiber Propagation Effects on Uncompensated Coherent Transmission Systems," *J. Lightwave Technol.,* vol. 35, pp. 458–480, 2017.
[34] A. Ferrari *et al.*, "GNPy: an open source application for physical layer aware open optical networks," *J. Opt. Commun. Netw.*, vol. 12, pp. c31-c40, 2020.
[35] P. Johannisson and E. Agrell. "Modeling of nonlinear signal distortion in fiber-optic networks," *J. Lightwave Technol.,* vol. 32, pp. 4544–4552, 2014.
[36] Discovery Semiconductors: https://www.discoverysemi.com/Product_Pages/Coherent/coherent_receivers.php
[37] P. Winzer, A. Gnauck, A. Konczykowska, F. Jorge, and J.-Y. Dupuy, "Penalties from In-Band Crosstalk for Advanced Optical Modulation Formats", in *European Conf. on Optical Communications (ECOC)*, 2011, paper Tu.5.B.7.